Interpolation within a Recruitment Manoeuvre using a Non-Linear Autoregressive Model of Pulmonary Mechanics

R. Langdon*, P.D. Docherty*, Y.S. Chiew*, Knut Möller, J.G. Chase***

** Department of Mechanical Engineering, University of Canterbury, Christchurch, 8140, New Zealand (Tel: +64 3 3642571; email: ruby.langdon@pg.canterbury.ac.nz)*

*** Institute of Technical Medicine, Furtwangen University, Villingen-Schwenningen, Germany. (Tel: +49(0)7720 307 4395)*

Abstract: Mathematical models that capture patient-specific information can enable personalised mechanical ventilation, improving care for patients in the intensive care unit (ICU). A nonlinear autoregressive (NARX) model that uses pressure dependent elastance, and multiple time dependent resistance coefficients has been fit to 25 patient data sets containing increasing PEEP steps. This model was more successful than a well-accepted first order model (FOM) at describing the shape of the airway pressure curve. In this study, the NARX model and FOM were identified on the first 20% and last 20% of the available data (IDD40). The parameterized model was then interpolated over the evaluation data (EVD) that consisted of the middle 60% of the data. The model-data residuals were compared to the result of identification using 100% of the data (IDD100). There were significant differences between the average root mean square (RMS) residuals for most IDD100, IDD40, and EVD combinations ($p < 0.05$). However, the magnitude of the differences was small in a clinical sense. Importantly, the NARX model was able to provide consistent results across all 25 patients. In contrast the FOM interpolation results were worse when the patient suffered over-distension in the high PEEP IDD40 data. The results suggest the NARX model could be suitable for use in the ICU, to estimate behaviour when data is not available, allowing clinicians to make informed decisions regarding ventilator PEEP settings.

Keywords: Autoregressive Models, Parameter Identification, Biomedical Systems, Nonlinear Systems

1. INTRODUCTION

Mechanical ventilation (MV) is an essential therapy for patients in the intensive care unit (ICU) suffering from acute respiratory distress syndrome (ARDS) (Girard and Bernard, 2007). ARDS is generally characterised as an inflammation in the lungs, and results in increased pulmonary elastance and inadequate oxygenation (Gattinoni *et al*., 2004). It is a heterogeneous condition that varies between patients. Hence, determination of optimal ventilator settings must be patient-specific (Brower *et al*., 2003, Pulletz *et al.*, 2012).

Positive end expiratory pressure (PEEP) is a ventilator setting that maintains positive airway pressure throughout the whole breathing cycle. PEEP helps to recruit new lung units, and prevent de-recruitment at the end of expiration (Meade *et al*., 2008). However, a suboptimal PEEP level can result in ventilator induced lung injury (VILI) (Dreyfuss and Saumon, 1998, Ricard *et al*., 2003). Such damage negates the positive effect of PEEP induced recruitment, further complicating patient condition, and repeating the cycle. In addition, when damage is caused to the lungs there is a release of inflammatory and other biological mediators that can lead to organ failure and increases the risk of mortality (Phua *et al*., 2009).

A lung model that captures patient-specific behaviour allows clinicians to select optimal ventilator settings for each individual patient (Chiew *et al.*, 2011). This individualised ventilation could reduce VILI, and reduce patient morbidity and mortality (Fenstermacher and Hong, 2004). However, several factors have limited the development of a successful model for this purpose. For a model to be successfully used in the ICU, it should be minimally invasive and avoid additional measurements beyond those that are available at the bedside, such as PEEP, and airway pressure / flow. Since the respiratory system is complex, simple models using only these inputs have been generally unable to capture all clinically relevant dynamics (Docherty *et al*., 2014).

Langdon *et al*. (2015) proposed a nonlinear autoregressive model (NARX) of the respiratory system. The NARX model has been successfully fit to pressure curves across increasing PEEP steps, for 25 patient data sets. This paper presents an extended validation of the work, where the NARX model is identified on the first and last 20% of data, and then interpolated to cover the middle 60%. This is valuable because complete data for the full range of PEEP steps may not always be available for each patient. Thus, having a method to estimate patient-specific respiratory mechanics when data is not available would provide clinicians with a more complete understanding of the individual patient's condition, and could potentially aid the selection of an optimal PEEP, or other MV settings. It is also a test of the NARX model's generality over the input range. The first order model (FOM) of pulmonary mechanics provided the basic structure upon which the NARX model was built, and was used as a comparison for the results.

2. MATERIALS AND METHODS

2.1 Data

The data was obtained from a study conducted in the ICUs of eight German hospitals between 2000 and 2002 (Stahl *et al.*, 2006). In this study, measurements were taken from 28 patients who suffered from acute lung injury and ARDS. A wide range of patient conditions were covered, as the patient age ranged from 17 to 77, and the cause of ARDS included a mix of lung and brain injuries. The protocol was approved by the ethics committee of each participating institution.

Airway pressure and flow were measured at the airway opening, using a pneumotachometer and piezoresistive transducer. The volume was then calculated from continuous integration of the flow, with adjustment for volume drift. Volume controlled ventilation was used, and an end inspiratory pause of ≥ 0.2 seconds was applied. During the study, patients underwent multiple recruitment manoeuvres. For this analysis, we have selected a portion of data from the patient data sets that spans 8 – 10 minutes. During this period, patients were ventilated at zero PEEP for approximately five minutes, and then PEEP was increased in steps of 2 cmH_2O after every 10 breathing cycles, until a peak inspiratory pressure of ~50 cmH_2O was reached.

This portion of the data was selected because of the large range of pressures covered, which enables the model's interpolation ability to be evaluated. The data also includes a number of PEEP steps and high maximum inspiratory pressure, providing the opportunity to test the model's ability to capture alveolar recruitment and, in some cases, nonlinear over-distension, which occur at different times and different pressures for each patient.

Data from 27 patients who participated in the study is available, and the analysis here was performed on 25 patients. The remaining two patients exhibited highly nonlinear behaviour that was most likely due to chronic obstructive pulmonary disease. The NARX model performed poorly on these two data sets (Langdon *et al.*, 2015), so they have been excluded from the cohort for the purpose of this analysis.

2.2 Respiratory Models

The first order model describes the respiratory system as a combination of one elastic and one resistive component:

$$P(t) = R\dot{V}(t) + EV(t) + P_0, \tag{1}$$

where P is the measured airway pressure (cmH_2O), t is time (s), R is the Poiseuille airway resistance (cmH_2Os/L), $\dot{V}$ is the airway flow rate, E is the pulmonary elastance (cmH_2O/L), V is the inspired volume (L), and P_0 is the offset pressure (cmH_2O), which is usually equal to PEEP.

The NARX model uses a similar structure to the FOM, but contains multiple resistance coefficients and incorporates multiple pressure dependent basis functions.

$$P(t) = \sum_{i=1}^{M} a_i \emptyset_{i,d}\big(P(t)\big)V(t) + \sum_{j=0}^{L} b_j \dot{V}(t_{-j}) + cP_0(t) \tag{2}$$

where a_i, b_j, and c are the parameters to be identified. M is the number of basis-functions to be used, $\emptyset_{i,d}$ is a particular basis function of degree d, a_i is the coefficient for a given basis function, and $\emptyset_{i,d}\big(P(t)\big)$ is the basis function value for a given pressure measurement. The sum of the basis functions multiplied by a_i represent elastance through pressure. There are L b_j coefficients, which represent the effect of airway resistance to flow and changes in flow. The FOM can be replicated with $M = L = c = 1$, and $d = 0$.

Zeroth order basis-functions ($d = 0$) are defined:

$$\emptyset_{i,0}(P) = \begin{cases} 1 & if\ P_i \le P < P_{i+1} \\ 0 & otherwise \end{cases} \tag{3}$$

where P_i are division points that subdivide the interval $0 \le P \le P_{max}$. Basis functions of higher degrees are defined recursively (de Boor, 1972):

$$\emptyset_{i,d}(P) = \frac{P - P_i}{P_{i+d} - P_i}\emptyset_{i,d-1}(P) + \frac{P_{i+d+1} - P}{P_{i+d+1} - P_{i+1}}\emptyset_{i+1,d-1}(P) \tag{4}$$

Fig. 1. shows five first order basis functions spanning the pressure range 0 – 50 cmH_2O. By definition, a first degree basis function overlaps with the two adjacent basis functions. Therefore the first and fifth basis functions are non-zero for half the range of pressures compared to basis functions two, three, and four.

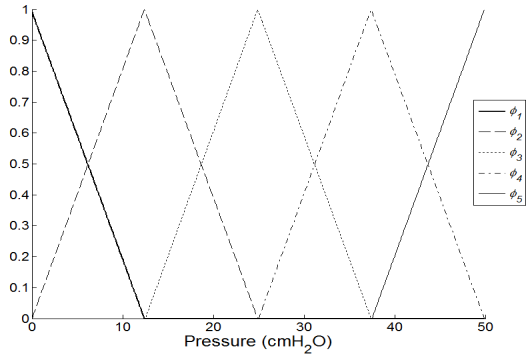

Fig. 1. First order basis functions for $0 \le P \le 50$ with $P_i \in [0, 12.5, 25, 37.5, 50]$ cmH_2O.

Previous work on the same data sets has shown that first degree basis functions provided an improvement over zeroth degree functions. However, there was no significant difference in outcomes for second degree functions (Langdon *et al.*, 2015). The analysis also determined that $L = 350$ was appropriate to enable the model to capture the end-inspiratory pause in the data, and $M = 5$ was appropriate due to the range of pressures that exist in the data (0 – 50 cmH_2O) (Langdon *et al.*, 2015). Therefore $d = 1$, $L = 350$, and $M = 5$ are used.

To identify the coefficients a_i, b_j, and c, (2) was evaluated throughout time to generate a matrix of equations:

$$\mathbf{Ax} = \mathbf{b} \tag{5}$$

where:

$$\mathbf{A} = \begin{bmatrix} \emptyset_{1,d}(P_{aw}(t_0))V(t_0) & \dots & \emptyset_{M,d}(P_{aw}(t_0))V(t_0) & \dot{V}(t_0) & \dots & \dot{V}(t_{-L}) & P_0(t_0) \\ \emptyset_{1,d}(P_{aw}(t_1))V(t_1) & \dots & \emptyset_{M,d}(P_{aw}(t_1))V(t_1) & \dot{V}(t_1) & \dots & \dot{V}(t_{L-j-2}) & P_0(t_1) \\ \vdots & \vdots & \vdots & \vdots & \vdots & \vdots & \vdots \\ \emptyset_{1,d}(P_{aw}(t_N))V(t_N) & \dots & \emptyset_{M,d}(P_{aw}(t_N))V(t_N) & \dot{V}(t_N) & \dots & \dot{V}(t_{N-L}) & P_0(t_N) \end{bmatrix}$$

$$\mathbf{b} = \begin{bmatrix} P_{aw}(t_0) \\ P_{aw}(t_1) \\ \vdots \\ P_{aw}(t_N) \end{bmatrix} \quad \text{and} \quad \mathbf{x} = \begin{bmatrix} a_1 \\ \vdots \\ a_M \\ b_1 \\ \vdots \\ b_L \\ c \end{bmatrix}$$

The coefficients (a_i, b_i, c) are found by solving:

$$\boldsymbol{x} = (\boldsymbol{A}^T\boldsymbol{A})^{-1}\boldsymbol{A}^T\boldsymbol{b} \tag{6}$$

Since measured data begins at time t_0, any elements with negative time were set to zero.

2.3 Analysis

The FOM and NARX model coefficients were identified using 40% of the available data for each patient. This identification data (IDD40) was composed from the concatenation of the first 20% and the last 20% of data. The pressures present in the IDD40 covered the full range of 0 – 50 cmH_2O, which provided adequate information for the identification of all five basis function coefficients. The IDD40 consisted of approximately 100 seconds of zero PEEP, and data from the highest PEEP levels encountered.

The remaining 60% was used as the evaluation data (EVD) to assess the interpolation capabilities of the models, identified from IDD40. The EVD consisted of 3 – 4 minutes of zero PEEP data, and approximately six increasing PEEP steps for each patient (Fig. 2). To quantify model performance, root mean square (RMS) residuals of the pressure fit were calculated separately for the IDD40 section and the EVD section. To provide a comparison, the models were also identified on 100% of the data (IDD100). The analysis was performed on an i7 quad core PC with 16GB RAM using 64 bit MATLAB, version 2014a (MathWorks, Natick, MA).

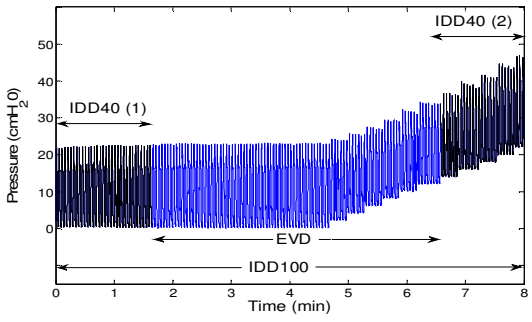

Fig. 2. Pressure identification data and evaluation data for one patient. IDD40 was composed from the concatenation of IDD40 (1) and IDD40 (2).

3. RESULTS

Table 1 shows the average of the RMS residuals across the 25 patient data sets. This information is also shown graphically in Fig. 3. The error bars overlap in all three cases for both models. Table 2 shows the p values resulting from paired signed rank tests. There is a significant difference in RMS residuals for most IDD100, IDD40, and EVD combinations at the 5% level.

Table 1. Mean RMS residuals and the 90% confidence intervals (cmH_2O).

	RMS Mean ± Standard Error and 90% Confidence Interval (CI)
NARX IDD100	0.93 ± 0.05 (CI: 0.83 – 1.03)
NARX IDD40	1.00 ± 0.06 (CI: 0.88 – 1.12)
NARX EVD	1.08 ± 0.07 (CI: 0.93 – 1.23)
FOM IDD100	1.72 ± 0.10 (CI: 1.53 – 1.91)
FOM IDD40	1.89 ± 0.11 (CI: 1.67 – 2.11)
FOM EVD	1.69 ± 0.10 (CI: 1.49 – 1.89)

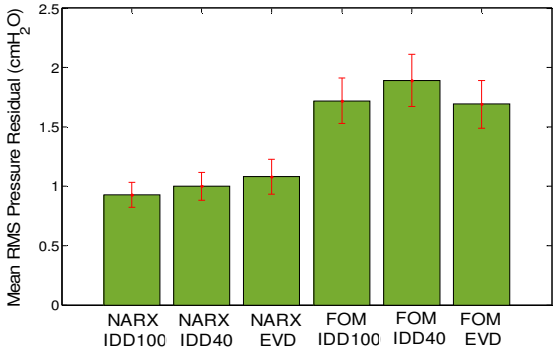

Fig. 3. Mean RMS residuals and 90% confidence intervals for the NARX and FOM, calculated from the identification data IDD100 and IDD40, and the evaluation data EVD.

Table 2. Paired signed rank test results for RMS comparison.

NARX		FOM	
IDD100, EVD	$p < 0.05$	IDD100, EVD	$p = 0.2$
IDD100, IDD40	$p < 0.05$	IDD100, IDD40	$p < 0.05$
IDD40, EVD	$p < 0.05$	IDD40, EVD	$p < 0.05$

Figs. 4 – 7 present results for two individual patient data sets, A and B. In these figures, the average breath in the IDD or EVD section is plotted. The mean residuals are then plotted relative to the average breath, at regularly spaced points. The error bars are the standard error. The first and second halves of IDD40 are denoted $IDD40_1$ and $IDD40_2$, respectively. Fig. 8 shows how the elastance coefficients for these patients change over pressure for the NARX with five basis functions, compared to the FOM with a single elastance coefficient.

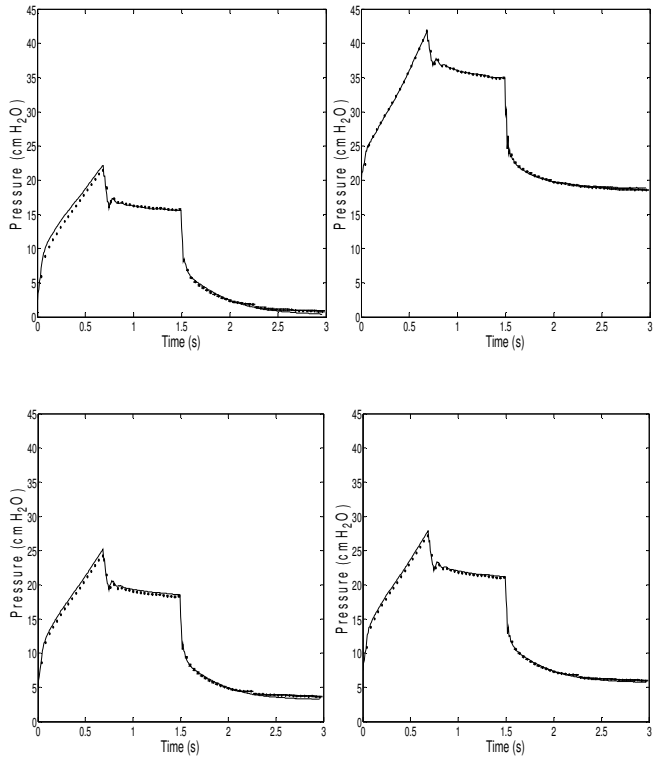

Fig. 4. Patient A, NARX model: $IDD40_1$ (top left), $IDD40_2$ (top right), EVD (bottom left), IDD100 (bottom right).

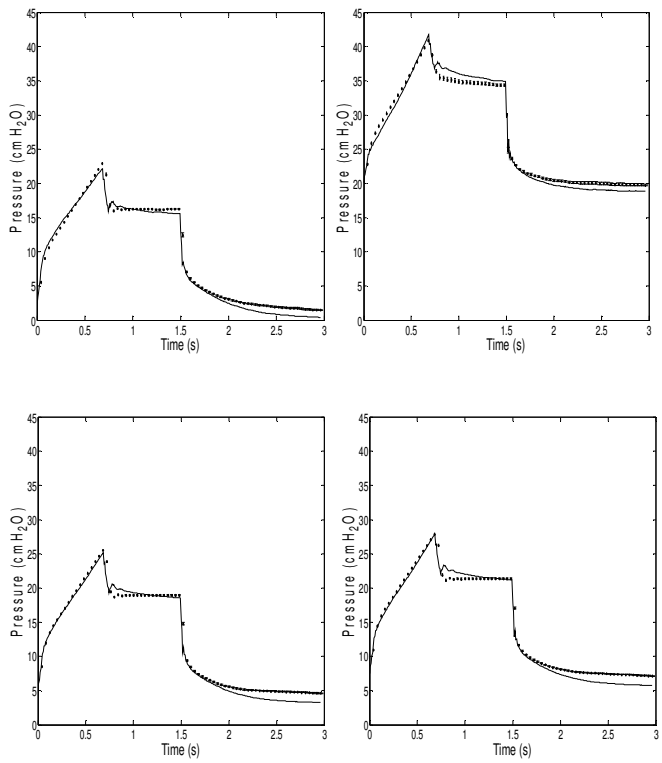

Fig. 5. Patient A, FOM: $IDD40_1$ (top left), $IDD40_2$ (top right), EVD (bottom left), IDD100 (bottom right).

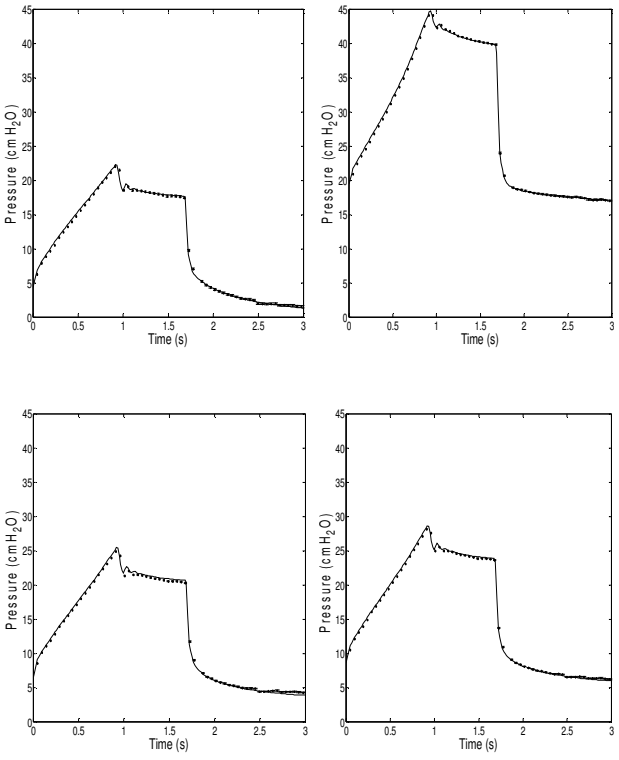

Fig. 6. Patient B, NARX model: $IDD40_1$ (top left), $IDD40_2$ (top right), EVD (bottom left), IDD100 (bottom right).

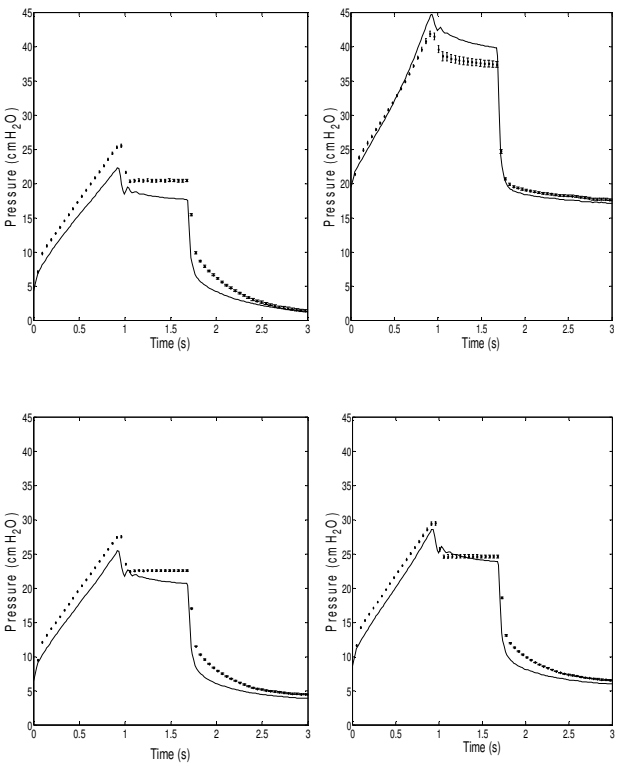

Fig. 7. Patient B, FOM: $IDD40_1$ (top left), $IDD40_2$ (top right), EVD (bottom left), IDD100 (bottom right).

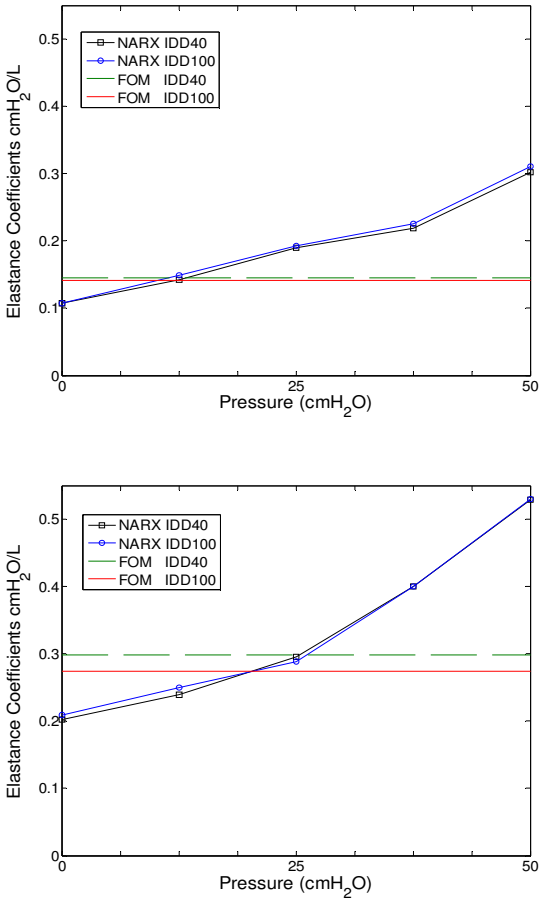

Fig. 8. Elastance coefficients identified on 40% or 100% of data, for patient A (top), and patient B (bottom).

The ΔP is defined as the difference between the maximum and minimum pressure within a breath. This value is relevant because changes in ΔP are indicative of changes in elastance in volume controlled mode. Both patients A and B began with a ΔP of approximately 22 cmH_2O at zero PEEP. For patient A, the ΔP remained constant until PEEP = 16 cmH_2O, and then slowly increased to a maximum of 26 cmH_2O at PEEP = 24 cmH_2O. For patient B, the ΔP was constant until PEEP = 10 cmH_2O, then increased rapidly to a maximum of 30 cmH_2O at PEEP = 20 cmH_2O, at the end of the recruitment manoeuvre. Each of the other 23 patients showed similar behaviour to either patient A or B.

3. DISCUSSION

Fig. 3 shows the average RMS residuals for the various identification and evaluation sections of data. The NARX results show that the residuals were smallest when the model was identified on 100% of the data, and largest when interpolated over the evaluation data, as expected. There were significant differences in RMS error across the IDD100, IDD40, and EVD for the whole cohort (signrank $p < 0.05$). However, the mean values are similar, and the 90% confidence intervals overlap for the three sections (Table 1). This result indicates that the outcome of interpolating the NARX model was not substantially worse than identifying the model on 100% of the data, for this group of 25 patients. Hence, the model can be effectively used to interpolate between measured, clinically relevant states.

For the FOM, the largest average residuals occurred for IDD40, and the smallest residuals occurred for EVD. This was because the ΔP tended to gradually increase over the course of the recruitment manoeuvre, and the FOM was unable to capture both the lower ΔP and higher ΔP that were both present in IDD40 with a single elastance. The parameter identification found a trade-off between the two states, resulting in high residuals for the whole IDD40 section. Since the ΔP in the EVD was generally in between the ΔP at the lowest and highest PEEPs, the trade-off allowed the FOM to be a better fit to the EVD section than the IDD40 section overall. The FOM IDD100 RMS residuals were slightly better than IDD40 on average because the model was fit to all of the data rather than just the extremes. There was a statistically insignificant difference between the FOM RMS residuals for IDD100 and EVD for this cohort (Table 2).

Similar to the NARX model result, the magnitude of the differences in RMS residuals for the FOM were not large. The 90% confidence intervals of the three cases overlapped, as shown in Table 1 and Fig. 3. However, there was clear evidence that the NARX model resulted in significantly lower residuals than the FOM. Lower residuals were achieved primarily because the NARX model was more successful than the FOM at capturing the lung relaxation during expiration and the end-inspiratory pause. This result is illustrated in Figs. 4 – 7, and was expected because the FOM is too simple to fully capture the complex behaviour described by this data, that incorporates viscoelastic effects.

Figs. 4 – 7 show results for two individual patients, A and B that represent the extremities of the range of ARDS patients tested. For patient B, the ΔP began increasing at a lower PEEP, and increased at a faster rate compared to patient A. The larger ΔP at the end of the recruitment manoeuvre was most likely caused by over-distension of some alveoli in the lungs of patient B. This important characteristic implies that patient B may be more at risk of VILI at lower pressures than patient A (Dreyfuss and Saumon, 1998).

For both patients A and B, most of the ΔP increases occurred in the final 20% of the data. Thus, the EVD pressure curves were more similar to those in the $IDD40_1$ section, so the FOM EVD residuals were similar to the $IDD40_1$ residuals. (Fig. 5, 7). For patient B, the more extreme ΔP increase in $IDD40_2$ caused the FOM to considerably overshoot the data in $IDD40_1$, capturing patient state comparatively poorly. Thus, the FOM EVD residuals for this patient are much larger than the IDD100 residuals. This result shows that in addition to failing to capture the end-inspiratory pause and expiration curve, the FOM is unsuitable for the type of interpolation performed here, when the patient exhibits over-distension at high PEEP levels. In contrast, there were no major differences between the IDD40, EVD, and IDD100 sections for the NARX model, for both patients A and B (Fig. 4, 6). Thus, the NARX model was capable of more accurate interpolation.

Fig. 8 shows the elastance coefficient results for the NARX model and FOM for patients A and B. The similarity of the NARX a_i coefficients shows that very similar models were

able to be identified for both patients using either 40% or 100% of the data. The result is also very similar for the FOM for patient A, but not for patient B, due to the over-distension present in the IDD40, as discussed above.

A limitation of interpolation with the NARX model is the fact that the range of pressures in the identification data must cover the entire interpolation range. If this was not the case, there may not be enough information to accurately identify one or more of the basis function coefficients. Similarly, the model may not be able to be extrapolated to pressures above or below the pressures encompassed by the basis functions. To overcome this limitation, a trend line could be fitted to the shape that is obtained by plotting the a_i coefficients. Extrapolation of this curve would allow the model to predict behaviour at higher or lower PEEP levels.

Model interpolation is valuable because data covering the full range of PEEP steps may not be available for some respiratory patients in the ICU. In practice, it is unlikely that clinicians would jump from zero PEEP to high PEEP without going through some intermediate stages. However, the results of this study are useful because it has proven that 60% of the recruitment manoeuvre data was not necessary to identify an accurate NARX model. This result could lead to the implementation of more efficient recruitment manoeuvres, wherein PEEP is increased as quickly as is safe for the patient. Having an accurate estimate of patient behaviour at all intermediate PEEP levels could then allow clinicians to make informed decisions about ventilator settings, and reduce risk of VILI.

The accuracy of the interpolation results using the NARX model suggest that it could be of use to clinicians, especially as it only requires measurements that are readily available at the bedside, and is identifiable in real-time. However, investigation of the method with a larger patient cohort and under different ventilation modes is necessary to fully evaluate the efficacy of the approach. It is possible that a clearer distinction between the IDD40, IDD100, and EVD residuals may be seen with a larger sample size.

5. CONCLUSION

The NARX model and FOM were identified on 40% of the data from 25 patients who underwent a recruitment manoeuvre, and interpolated over the remaining 60% of data. The NARX model was more successful than the FOM at fitting to the EVD, primarily because it was able to better capture the end-inspiratory and expiratory relaxation in each breathing cycle. The NARX model was particularly superior in cases where the data suggested over-distension was occurring at high PEEP levels. The consistency of the NARX model interpolation for both type A and B patients suggests it could be successfully used with a wide range of ARDS patients with different disease characteristics. Since each patient and their disease state are different, this property is essential for a model to be useful in practice.

REFERENCES

Brower, R. G., Morris, A., Macintyre, N., Matthay, M. A., Hayden, D., Thompson, B. T., Clemmer, T., Lanken, P. N., Schoenfeld, D., Natl Inst, H., Network, A. C. T. and Natl Heart Lung Blood, I. (2003). Effects of recruitment maneuvers in patients with acute lung injury and acute respiratory distress syndrome ventilated with high positive end-expiratory pressure. *Critical Care Medicine,* volume 31**,** 2592-2597.

Chiew, Y. S., Chase, J. G., Shaw, G. M., Sundaresan, A. and Desaive, T. (2011). Model-based PEEP optimisation in mechanical ventilation. *Biomedical engineering online,* volume 10**,** 111-111.

De Boor, C. (1972). On calculating with B-splines. *Journal of Approximation Theory,* volume 6**,** 50-62.

Docherty, P. D., Schranz, C., Chiew, Y.-S., Möller, K. and Chase, J. G. (2014). Reformulation of the pressure-dependent recruitment model (PRM) of respiratory mechanics. *Biomedical Signal Processing and Control,* volume 12**,** 47-53.

Dreyfuss, D. and Saumon, G. (1998). Ventilator-induced Lung Injury. Lessons from Experimental Studies. *Am J Respir Crit Care Med,* volume 157**,** 294 - 323.

Fenstermacher, D. and Hong, D. (2004). Mechanical ventilation: what have we learned? *Critical Care Nursing Quarterly,* volume 27**,** 258-294.

Gattinoni, L., Chiumello, D., Carlesso, E. and Valenza, F. (2004). Bench-to-bedside review: Chest wall elastance in acute lung injury/acute respiratory distress syndrome patients. *Critical Care,* volume 8**,** 350 - 355.

Girard, T. D. and Bernard, G. R. (2007). Mechanical ventilation in ARDS: A state-of-the-art review. *Chest,* volume 131**,** 921-929.

Langdon, R., Docherty, P. D., Chiew, Y. S., Moeller, K. and Chase, J. G. (2015). Use of basis functions within a non-linear autoregressive model of pulmonary mechanics. *BioMed Research International,* In Review.

Meade, M. O., Cook, D. J., Griffith, L. E., Hand, L. E., Lapinsky, S. E., Stewart, T. E., Killian, K. J., Slutsky, A. S. and Guyatt, G. H. (2008). A Study of the Physiologic Responses to a Lung Recruitment Maneuver in Acute Lung Injury and Acute Respiratory Distress Syndrome. *Respiratory Care,* volume 53**,** 1441-1449.

Phua, J., Badia, J. R., Adhikari, N. K. J., Friedrich, J. O., Fowler, R. A., Singh, J. M., Scales, D. C., Stather, D. R., Li, A., Jones, A., Gattas, D. J., Hallett, D., Tomlinson, G., Stewart, T. E. and Ferguson, N. D. (2009). Has Mortality from Acute Respiratory Distress Syndrome Decreased over Time?: A Systematic Review. *American Journal of Respiratory and Critical Care Medicine,* volume 179**,** 220-227.

Pulletz, S., Adler, A., Kott, M., Elke, G., Gawelczyk, B., Schädler, D., Zick, G., Weiler, N. and Frerichs, I. (2012). Regional lung opening and closing pressures in patients with acute lung injury. *Journal of critical care,* volume 27**,** 323.e11.

Ricard, J. D., Dreyfuss, D. and Saumon, G. (2003). Ventilator-induced lung injury. *Eur Respir J,* volume 22**,** 2s-9.

Stahl, C. A., Möller, K., Schumann, S., Kuhlen, R., Sydow, M., Putensen, C. and Guttmann, J. (2006). Dynamic versus static respiratory mechanics in acute lung injury and acute respiratory distress syndrome. *Critical Care Medicine,* volume 34**,** 2090-2098.